Journal of Zhejiang University-SCIENCE A (Applied Physics & Engineering)
ISSN 1673-565X (Print); ISSN 1862-1775 (Online)
www.jzus.zju.edu.cn; www.springerlink.com
E-mail: jzus@zju.edu.cn

Urban railway ground vibrations induced by localized defects: using dynamic vibration absorbers as a mitigation solution*

Georges KOUROUSSIS†[1], Sheng-yang ZHU[2], Bryan OLIVIER[1], Daniel AINALIS[3], Wan-ming ZHAI[2]

[1]*Department of Theoretical Mechanics, Dynamics and Vibrations, University of Mons, Mons 7000, Belgium*

[2]*State Key Laboratory of Traction Power, Train and Track Research Institute, Southwest Jiaotong University, Chengdu 610031, China*

[3]*Center for Transport Studies, Department of Civil and Environmental Engineering, Imperial College London, London SW7 2AZ, UK*

†E-mail: georges.kouroussis@umons.ac.be

Received Nov. 23, 2018; Revision accepted Dec. 28, 2018; Crosschecked Jan. 7, 2019

Abstract: Recent increases in urban railway track infrastructure construction are often delayed by distress to occupants caused by ground-borne vibration arising from the passing of the rail vehicle. Mitigation measures are proposed as a solution if they prove their efficiency in reducing these vibrations. In this paper, we present a practical study of dynamic vibration absorbers (DVAs) as a possible measure. A complete numerical study based on a recently developed two-step approach is performed. A detailed multibody model for the vehicle is coupled to a finite element/lumped mass model for the track in order to predict the forces acting on the soil. Then a 3D finite element model of the soil simulates the ground wave propagation generated from these dynamic forces to evaluate the level of vibration in the surrounding area. Having validated this model in the past, it is used to determine the effectiveness of DVA placed either in the vehicle or on the track. Compared to existing studies presenting DVA calibrations in terms of frequency response functions, realistic simulations are presented, based on the specific case of the T2000 tram circulating in Brussels traversing a localized defect. The results demonstrate that a DVA placed on the vehicle remains an interesting solution, provided that the mass is sufficient (mass ratio of 0.1).

Key words: Dynamic vibration absorber; Turnout; Rail joint; Ground vibration; Brussels tram
https://doi.org/10.1631/jzus.A1800651 **CLC number:** U213

1 Introduction

In the development of railway lines in the urban environment or during network extensions, railway-induced ground vibration remains an important showstopper. Residents are generally adverse to such developments as significant levels of vibration are often felt and can affect their daily lives. The role of engineers, either as a designer in train dynamics or as a railroad supervisor, should be to ensure that all the preventive actions were taken to minimize the generated vibrations. However, mitigation measures were also applied during network operation, after having observed important vibration levels (Vogiatzis, 2012; Licitra et al., 2016). This is one of the reasons that mitigation solutions are classified by actions on the source (vehicle) or on the receptor (trackbed). The use of prediction models offers an efficient approach

* Project supported by the Overseas Expertise Introduction Project for Discipline Innovation (111 Project) of China (No. B16041)
ORCID: Georges KOUROUSSIS, https://orcid.org/0000-0002-9233-1354
© Zhejiang University and Springer-Verlag GmbH Germany, part of Springer Nature 2019

to estimate the potential reduction of vibration prior to any physical intervention. Such tools are currently the focus of a large body of research (Connolly et al., 2016).

Three contributions to ground vibration are generally retained to characterize the source of vibration (Kouroussis et al., 2014):

1. The moving load effect (called quasi-static contribution), which represents the response of a structure to moving vehicles where only the axle loads are considered.

2. The roughness distributed along the track (generating a dynamic contribution where the vehicle dynamics play a minor role).

3. The possible localized defect(s) as a rail joint or turnout (also a dynamic contribution where the vehicle dynamics play a major role).

Contributions 1 and 2 are the most studied effects since detailed modeling of the vehicle is generally not required. However, contribution 3 primarily depends on the vehicle characteristics, and to a lesser extent, the trackbed characteristics.

Singular geometrical imperfections are key in the associated studies, based on an accurate description of the interaction between the track and the vehicle, and take into account the various components of the track/foundation system. The impact forces on the wheel/rail contact area have received considerable attention, focusing on turnouts (Bruni et al., 2009), permanently dipped rail joints (Mandal et al., 2016), multiple wheel flats (Uzzal et al., 2016), wheel polygonalization (Nielsen et al., 2015), or rail joints (Grossoni et al., 2015). Kouroussis et al. (2010) showed that the vehicle signature (eigen modes) is present in the generated ground vibration for the vehicle passing over a rail joint; using a prediction model working in two successive steps, it was demonstrated that the ground vibration was completely different (level and shape) when considering a detailed model instead of a set of loaded wheelsets to represent the vehicle. This approach has also been used to analyze resilient wheels and their effect on the generated ground vibration levels in free-field (Kouroussis et al., 2012) or on the built environment (Kouroussis et al., 2013). Nielsen et al. (2015) suggested a reduction of unsprung masses and proved that such a measure minimizes wheel polygonalization or wheel flat. Kouroussis et al. (2018) proposed a hybrid numerical-experimental method to evaluate the vibration transmission initiated by rail defects; five defect types were studied and a sensitivity analysis was performed with respect to the studied site and speed.

Other research focused on the railway infrastructure. Vehicle/track interaction has received considerable attention in recent years and several numerical frameworks emerged to investigate the dynamics of the whole vehicle/track system (Zhai et al., 2009; Cai et al., 2019). Talbot (2014) studied specific geometry of localized defects (lift-over crossings) to minimize vibrations transmitted in sensitive buildings. Paixão et al. (2015) focused on transition zones to avoid abrupt changes in the vertical stiffness of the tracks. Germonpré et al. (2018) developed a numerical two-and-half model dedicated to geo-characteristic variation in the longitudinal direction with application to a transition zone between a ballasted and slab track. Coulier et al. (2013) proposed a subgrade stiffening system located close to the track to mitigate railway induced vibrations through the use of numerical methods. Vogiatzis and Mouzakis (2018) performed a large-scale experimental campaign in the city of Athens with the aim of evaluating the effect of building type and floating slab solutions as potential mitigation measures for the Athens metro (Vogiatzis, 2012; Vogiatzis et al., 2018). Connolly et al. (2013) investigated the relationship between trench geometry and vibration isolation performance. A detailed evaluation of mitigation methods dedicated to track and soil systems was recently conducted by Kaewunruen and Martin (2018), with the aim of life-cycle performance analysis. Many of these studies met the aforementioned classification (mitigation at the source or on the receptor). However, the first solution was less studied and mitigation solutions dedicated to the vehicle remain scarce. In addition, it is observed that modern numerical models have reached a level of maturity and can be widely used to simulate the efficiency of possible mitigation solutions, i.e. virtual prototyping.

The objective of this paper is to analyze the efficiency of dynamic vibration absorbers (DVAs) using a numerical prediction scheme that has been validated in recent work. DVAs can be tuned to a specific excitation frequency in order to reduce the forced response by absorbing the corresponding vibration resonance. In addition, the evaluation of the

best location of the DVA (vehicle or track) is also investigated for a significant gain in terms of ground vibration level reduction. To illustrate this study, the T2000 tram circulating in the Brussels transport network will be studied, for which several quantitative results are available and a means of vibration reduction is required.

2 Review of recent applications of dynamic vibration absorbers in the railway industry

In recent years, DVA systems have been widely used in railway engineering with various designs and aims employing unique advantages including design simplicity, high reliability, excellent performance, and simple maintenance. To emphasize the interest of DVA use in the present application, it could be relevant to enumerate recent applications, including the negative effect to be reduced and the type of track analyzed. Table 1 identifies some relevant DVA developments and classifies them as a function of the railway application.

Zhu et al. (2017a, 2017b) developed a novel railway track capable of attenuating low-frequency system vibrations using DVAs based on comprehensive theoretical and experimental analyzes, providing a valuable contribution to the issue of underground train-induced vibrations. Grassie and Elkins (1997) studied rail corrugation on North American metros, and found a significant reduction in rail corrugation is possible if a DVA is used to detune and damp the relevant mode of vibration. Collette et al. (2009) presented a dynamic vibration absorber tuned to the first torsional resonance of the wheel set, as a potential solution to mitigate rutting corrugation, and its efficiency has been demonstrated numerically and experimentally. Morys and Kuntze (1997) proposed to reduce the formation of polygonal wheels by active compensation through a mechatronic component that included a DVA. Thompson et al. (2007) designed a mass-spring-damper DVA with multiple tuning frequencies, and experimental results showed promising reductions of track component noise of around 6 dB. Vincent et al. (1996) adopted DVAs to increase the attenuation rate of rail vibrations, finding that, for ballasted track with bi-bloc concrete sleepers, the implementation of DVAs on the rail could result in a 2–6 dB reduction in track sound power. Gong et al. (2013) proposed to use a DVA attached under the chassis to mitigate the resonant vibration of the flexible car body. Simulation results revealed that the DVAs can achieve good reductions in vibration if optimal tuning according to the target frequencies of the car body is performed. Chen et al. (2019) established a detailed train-track-bridge coupled dynamic model with an attached bridge-based DVA, and investigated the influence of the bridge-based DVA on running trains under earthquake excitation.

This review demonstrates the possibilities of using DVAs in the railway industry and their effective location: often, a reduction of vibration in the vehicle or in the track implies the placement of a DVA on the system to be studied.

3 Vibration induced by the T2000 tram

Presenting the T2000 tram as a case study is relevant. This is an exemplary case of a vehicle generating high levels of vibration when the vehicle passes through obstacles like turnouts, crossings, or rail joints. The vehicle consists of three cars: two leading cars at the extremities and one central car (Fig. 1). Developed by Bombardier Transport, the T2000 tram is characterized by a low floor design made possible by dedicated bogies with independent rotating wheels and motors mounted inside

Table 1 Review of recent DVA/track development

Study	Effect to reduce	Application
Chen et al., 2019	Bridge vibration	Railway bridge
Zhu et al., 2017a, 2017b	Amplification area induced by floating slab	Underground lines
Gong et al., 2013	Car body resonance	High-speed trains
Collette et al., 2009	Rutting corrugation	Train wheel sets
Thompson et al., 2007	Track noise	At-grade tracks
Grassie and Elkins, 1997	Rail corrugations	Metro lines
Morys and Kuntze, 1997	Polygonal wheels	Train wheel sets
Vincent et al., 1996	Track noise	At-grade tracks

the wheels. The motorized wheels are also equipped with resilient wheels. As soon as the T2000 trams began operating in the Brussels tramway network, it was observed that the tram generated abnormal vibrations compared to other vehicles circulating on the same lines. Some studies (de Roeck et al., 1996; Kouroussis et al., 2010) have been conducted to propose solutions to alleviate the vibratory levels. From these studies, the following information can be ascertained:

1. A thorough investigation of the vehicle characteristics (masses and suspensions stiffness and damping) was carried out, and track and soil dynamic properties were obtained from in-situ test. These are presented in (Kouroussis et al., 2012).

2. The origin of high-level vibration was emphasized: the presence of the motor inside the wheel increases the unsprung masses and produces a strong dynamic interaction between the vehicle and the track, especially when the vehicle traverses significant track unevenness.

The prediction model adopted in this study is described by Kouroussis and Verlinden (2013), summarized as follows:

1. The vehicle model is built using an in-house multibody simulation tool. Fig. 2 shows the dynamic model adopted for the T2000 tram. A classical layout is used: car bodies, bogies, and wheel set are considered as rigid bodies (of mass m_i, $i = \mathrm{c}, \mathrm{b}, \mathrm{m}, \text{or } \mathrm{d}$) and are interconnected by the primary and secondary suspension systems (k_i and c_i for stiffness and damping coefficient, $i = 2, \mathrm{m}, \text{or } \mathrm{d}$). The particularity of this model lies in the presence of resilient wheels (for the motorized wheel) characterized by a rubber layer inserted between the web and the tread and composed of viscoelastic pads arranged in pairs circumferentially. This corresponds to a wheel set model with a stiffness k_t and damping coefficient c_t, and web mass designated by m_t.

2. The track is ballasted and modeled in two dimensions, using Euler-Bernoulli beam finite elements for the rail (Fig. 3). The rail pad, sleepers, and ballast are modeled using a series of lumped masses (m for the sleepers), springs (k_r and k_b for rail pad and ballast stiffnesses, respectively), and dampers (c_r and c_b for the damping coefficients). The soil supporting the flexible track model is incorporated using a coupled lumped mass (CLM) model, in the vertical plane (Kouroussis and Verlinden, 2015). Frequency independent, analytical expressions are used to replicate the behavior of a half-space. Five parameters (mass m_f, damping c_f and c_c, and stiffness k_f and k_c elements) define the CLM model and are obtained by fitting the corresponding soil response with respect to the dynamic soil parameters.

3. The coupling between the vehicle and the track is obtained using traditional Hertzian theory, including the geometry of the potential defects. To do this, a pre-processing step is used to solve the 3D contact problem to tabulate the values of the contact nonlinear spring coefficient according the position of the wheel with respect to the defect shape (Kouroussis et al., 2015).

4. The response of the ground is simulated using the commercial software ABAQUS. Special consideration is given to the definition of the boundary conditions to obtain the best representation of the domain infinity and, in particular, to avoid wave reflection.

5. The simulation of the complete model is

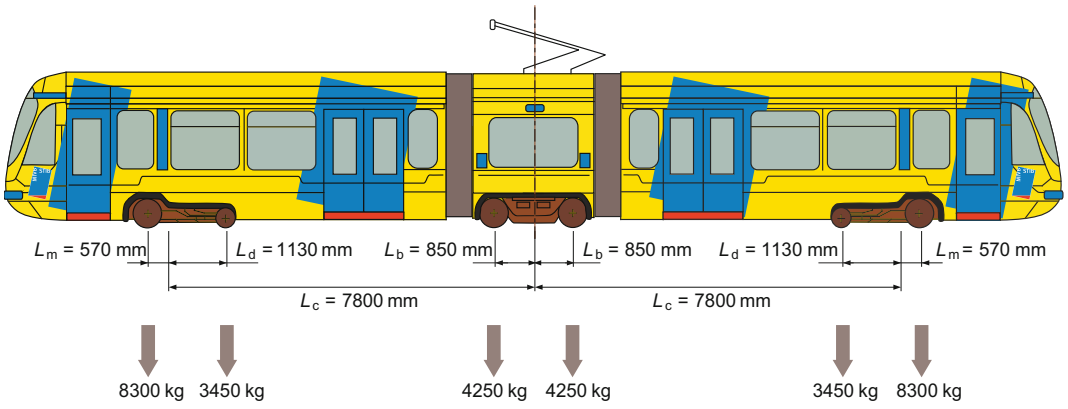

Fig. 1 Main dimensions and axle loads of the T2000 tram

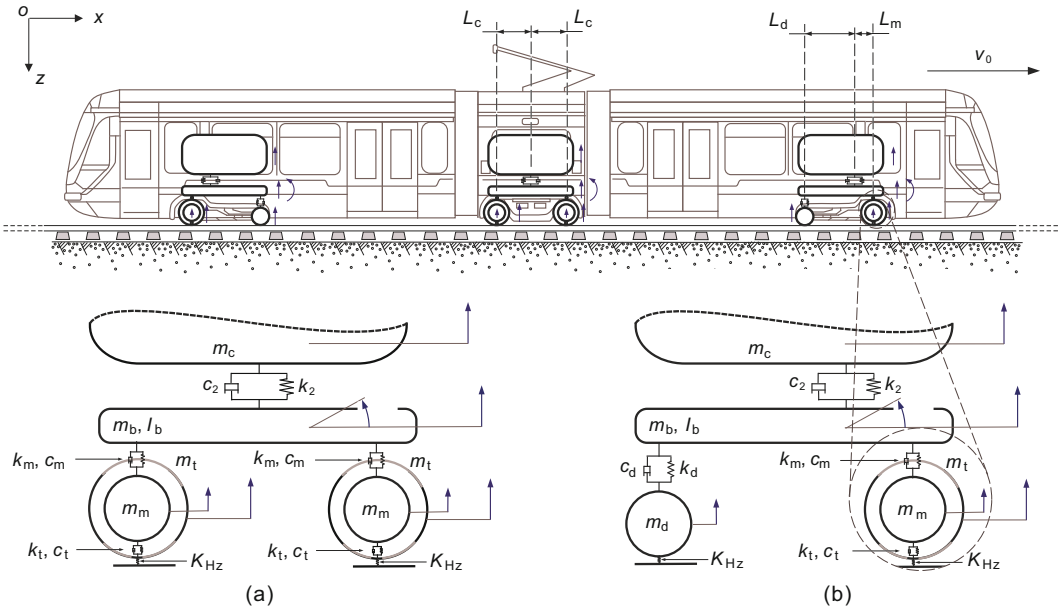

Fig. 2 T2000 tram numerical modeling approach: (a) central bogie modeling; (b) leading bogie modeling (I_b is the pitch inertia, and K_{Hz} is the Hertz contact non-linear stiffness)

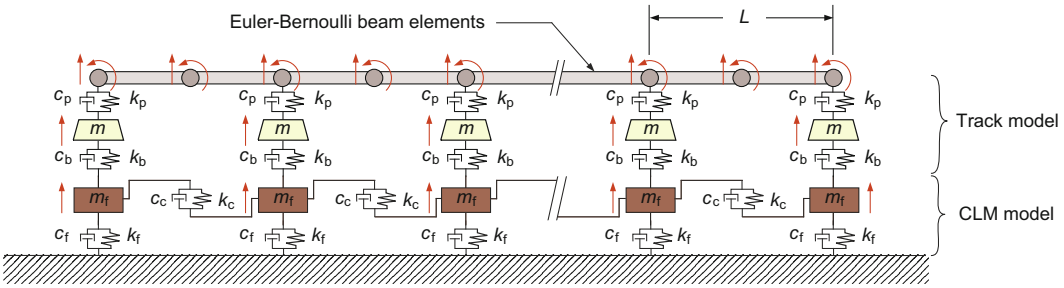

Fig. 3 Track/foundation coupling

performed in the time domain and in two successive steps: the vehicle/track/foundation subsystem is simulated first, and the time history of the forces exerted by the track on the soil is the output. Second is the simulation of the response of the soil to these forces using a finite element model. Numerical values of vehicle, track, and soil parameters are presented in Appendix A.

Fig. 4 shows an example of the simulated results obtained in the case of the vehicle running at a constant speed v_0 of 30 km/h and considering a localized defect representing a rail joint (rectangular shape of 1-mm height and 5-mm length). Such dimensions were fixed allowing a validation step with an artificial geometry and corresponding to typical values of defects encountered in practice (Kouroussis et al., 2010). The wheel/defect contact force (Fig. 4a) and the soil surface velocity at 2 m (Fig. 4b) are retained. This comparison allows for the correlation of impact forces and generated ground vibrations at each time instant: it is evident that the observed high-levels of vibration occur when the vehicle passes over the singular defect.

For transient phenomena, stationary analysis fails to identify the main frequencies that are excited. To overcome this, time-frequency analysis methods are preferred. Ainalis et al. (2018) suggested using the continuous wavelet transform that allows for the estimation of the localized dominant frequency for various phenomena producing ground vibration. Fig. 5 shows the corresponding time-frequency to the time history in Fig. 4. It is shown that, at each wheel/defect contact, the excitation amplitude covers a broad frequency range and, at the same

time (roughly the delay between excitation and response), the soil vibration amplitude is at maximum around 20–25 Hz. This is confirmed by recent research (Kouroussis et al., 2012) demonstrating that particular vehicle's modes, namely the bogie's pitch and bounce modes, are the primary contributors to the track and soil vibrations generated by the passing of the tram over an artificial rail joint. Table 2 shows the different mode shapes of the vehicle, obtained by linearizing the vehicle/track equations of motion around the nominal position. Comparing the modes with Fig. 5b, this confirms that the bogie bounce mode is responsible for the high vibration level.

The proposed model can be used as a basis to design a DVA (dynamic parameter and location) to evaluate its effectiveness for vibrations generated by dynamic and non-stationary excitations, amplified by the vehicle dynamics.

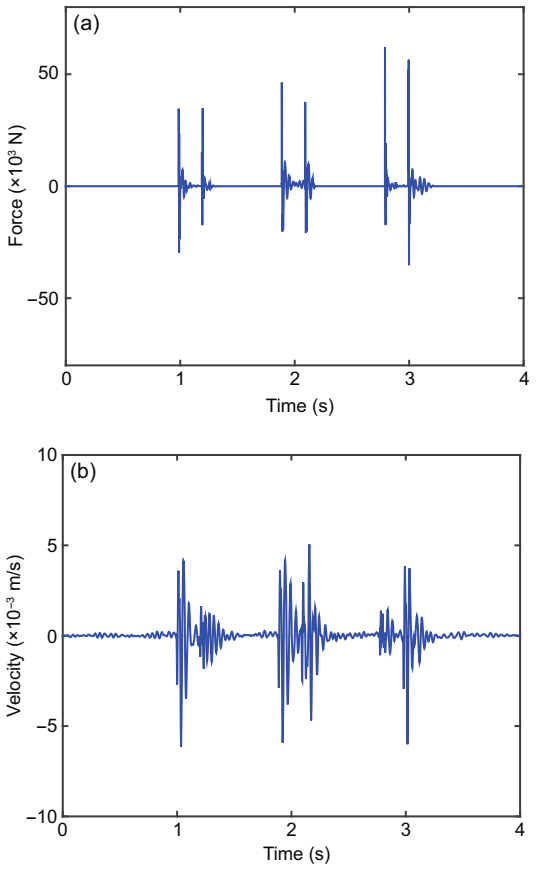

Fig. 4 Numerical results of the T2000 tram passing over a singular defect at a speed of 30 km/h: (a) time history of wheel/rail contact force; (b) time history of vibration velocity at 2 m from the track

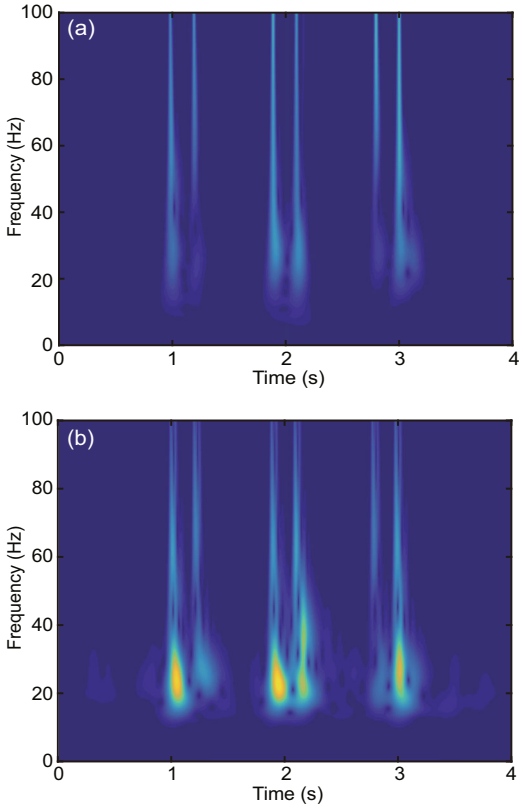

Fig. 5 Time-frequency velocity amplitude analysis corresponding to Fig. 4: (a) force amplitude; (b) velocity amplitude at 2 m from the track

4 Mitigation measures for urban railway-induced ground vibrations using dynamic vibration absorbers

4.1 Optimizing and calibrating DVA

Physically speaking, a DVA is a passive device that can be schematically expressed as a mass (m_a), connected to the system to be studied (usually named primary system) through a spring element (stiffness k_a) and a damper (damping coefficient c_a). If these parameters are tuned accordingly (Den Hartog, 1985), a DVA is capable of mitigating vibrations at a specified frequency, as those presented in Section 3. A DVA is thus widely accepted in vibration as one of the most suitable ways to suppress undesirable low-dampened resonance.

The concept is based on the coupling between the primary system and the DVA, each of them being described by a set of equations for the vehicle/track subsystem:

$$\boldsymbol{M}_\mathrm{p}\ddot{\boldsymbol{x}}_\mathrm{p} + \boldsymbol{C}_\mathrm{p}\dot{\boldsymbol{x}}_\mathrm{p} + \boldsymbol{K}_\mathrm{p}\boldsymbol{x}_\mathrm{p} = \boldsymbol{f}_\mathrm{p}, \tag{1}$$

Table 2 Main mode shapes of the T2000 tram: natural frequency $f_{0,i}$ and damping ratio ξ_i of mode i (taking into account the track flexibility)

Mode	Leading car	Central car
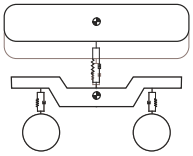 Car bounce	$f_{0,1}=1.8$ Hz ($\xi_1=32\%$)	$f_{0,1}=3.1$ Hz ($\xi_1=55\%$)
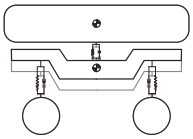 Bogie bounce	$f_{0,2}=19.6$ Hz ($\xi_2=14\%$)	$f_{0,2}=22.3$ Hz ($\xi_2=11\%$)
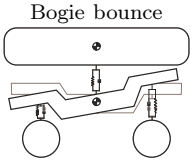 Bogie pitch	$f_{0,3}=29.1$ Hz ($\xi_3=8\%$)	$f_{0,3}=34.3$ Hz ($\xi_3=3\%$)
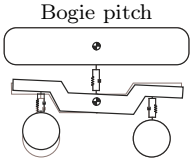 Axle hop	$f_{0,4}=45.5$ Hz ($\xi_4=9\%$)	$f_{0,4}=46.4$ Hz ($\xi_4=9\%$)

and for the DVA:

$$m_{\mathrm{a}}\ddot{x}_{\mathrm{a}}+c_{\mathrm{a}}\dot{x}_{\mathrm{a}}+k_{\mathrm{a}}x_{\mathrm{a}}=0, \tag{2}$$

where $\boldsymbol{M}_{\mathrm{p}}$, $\boldsymbol{C}_{\mathrm{p}}$, and $\boldsymbol{K}_{\mathrm{p}}$ are the mass, damping, and stiffness matrices of the primary system, respectively. Vector $\boldsymbol{x}_{\mathrm{p}}$ represents the set of configuration parameters defining the motion of the primary system and $\boldsymbol{f}_{\mathrm{p}}$ contains the forces acting on the system (excitation). The DVA motion is represented by x_{a}. When both systems are coupled, a single set of equations is retained

$$\boldsymbol{M}\ddot{\boldsymbol{x}}+\boldsymbol{C}\dot{\boldsymbol{x}}+\boldsymbol{K}\boldsymbol{x}=\boldsymbol{f}, \tag{3}$$

where all the masses, stiffness, and damping coefficients are included in the mass matrix $\boldsymbol{M}$, damping matrix $\boldsymbol{C}$, and stiffness matrix $\boldsymbol{K}$. All structure coordinates are defined by vector $\boldsymbol{x}$, while vector $\boldsymbol{f}$ contains the excitation forces.

Fig. 6 shows the proposed problem to be studied considering the vehicle/track subsystem as the primary system and the DVA attached to either the vehicle (case 1) or the track (case 2). For the latter scenario, two possible subcases could be considered: the DVA attached to the rail or to a single sleeper.

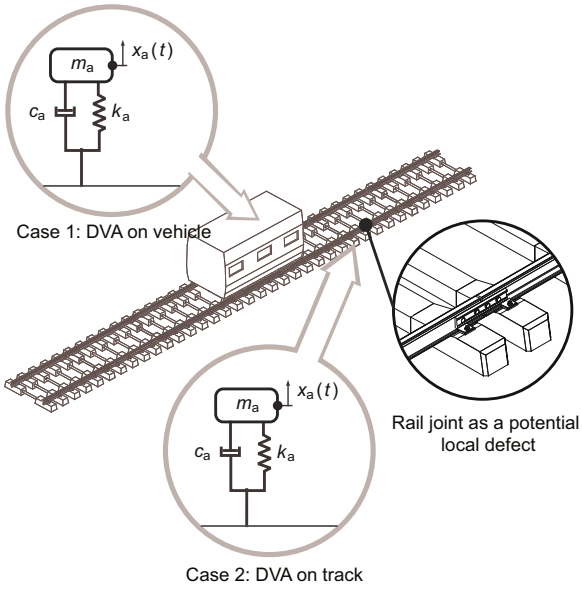

Fig. 6 Schematic representation of a damped dynamic vibration absorber attached to the vehicle/track system

For both configurations, the location of the DVA is obviously expected to be close to the localized defect.

The proposed approach is based on the modal decomposition of Eq. (3) applied to DVA analysis, as found in the literature (Steffen Jr and Rade, 2001). This allows each mode n of the primary system to be analyzed separately and to consider each of them as a single degree-of-freedom in the modal basis. To perform this, coordinate $x_f(t)$ of the applied excitation $f(t)$ and coordinate $x_c(t)$ of DVA connection node from vector $\boldsymbol{x}$ are rewritten with respect to the generalized coordinate $c_n(t)$ of mode n considered:

$$x_f(t)=\psi_{fn}\,c_n(t), \tag{4}$$

$$x_c(t)=\psi_{cn}\,c_n(t), \tag{5}$$

where ψ_{cn} and ψ_{fn} designate the cth and fth components of the eigenvector $\boldsymbol{\psi}_n$ of mode n. The modal orthogonality property allows the decoupling of Eq. (3), so that for the mode n, the decoupled equations are obtained:

$$m_n\ddot{c}_n+c_{\mathrm{a}}\psi_{cn}^2\dot{c}_n-c_{\mathrm{a}}\psi_{cn}\dot{x}_{\mathrm{a}}+(m_n\omega_n+k_{\mathrm{a}}\psi_{cn}^2)c_n -k_{\mathrm{a}}\psi_{cn}x_{\mathrm{a}}=\psi_{fn}f(t), \tag{6}$$

$$m_{\mathrm{a}}\ddot{x}_{\mathrm{a}}+c_{\mathrm{a}}\dot{x}_{\mathrm{a}}-c_{\mathrm{a}}\psi_{cn}\dot{c}_n+k_{\mathrm{a}}x_{\mathrm{a}}-k_{\mathrm{a}}\psi_{cn}c_n=0, \tag{7}$$

where the generalized mass m_n and the natural circular frequency ω_n are defined as

$$m_n=\boldsymbol{\psi}_n^{\mathrm{T}}\boldsymbol{M}\boldsymbol{\psi}_n, \tag{8}$$

$$m_n\omega_n^2=\boldsymbol{\psi}_n^{\mathrm{T}}\boldsymbol{K}\boldsymbol{\psi}_n. \tag{9}$$

To avoid any dependency with respect to the normalization procedure adopted for the eigenvector $\boldsymbol{\psi}_n$, it is preferable to introduce the effective mass $m_{n,\text{eff}}$ and effective stiffness $k_{n,\text{eff}}$:

$$m_{n,\text{eff}} = \frac{m_n}{\psi_{cn}^2}, \quad k_{n,\text{eff}} = \frac{m_n \omega_n^2}{\psi_{cn}^2}, \tag{10}$$

which also gives information about mode participation. Combining Eqs. (5)–(7), the primary response in the frequency domain provides the frequency response function (FRF), useful to analyze the amplitude response (Eq. (11)),

$$\begin{aligned}\frac{|X_c|}{F_0} =& \frac{\psi_{cn}\psi_{fn}}{k_{n,\text{eff}}} \left[(2\xi_n \Omega)^2 + (\Omega^2 - \varphi^2)^2\right]^{1/2} \\ & / \{(2\xi_n \Omega)^2 (1 - \Omega^2 - \mu_n \Omega^2)^2 \\ & + [\mu_n \varphi^2 \Omega^2 - (\Omega^2 - 1)(\Omega^2 - \varphi^2)]^2\}^{1/2},\end{aligned} \tag{11}$$

where

$$\begin{cases} \Omega = \dfrac{\omega}{\omega_n} & \text{(forcing frequency ratio)}, \\ \varphi = \dfrac{\omega_\text{a}}{\omega_n} & \text{(tuning factor)}, \\ \mu_n = \dfrac{m_\text{a}}{m_{n,\text{eff}}} & \text{(mass ratio)}, \\ \xi_n = \dfrac{c_\text{a}}{2 m_\text{a} \omega_n} & \text{(damping ratio)}, \end{cases} \tag{12}$$

with $\omega_\text{a} = \sqrt{k_\text{a}/m_\text{a}}$ the natural circular frequency of the DVA and X_c and F_0 the Fourier transform of $x_c(t)$ and $f(t)$, respectively. Optimal values φ_opt of the tuning factor and ξ_opt of the damping ratio provide the best attenuation and are key to maximizing the attenuation capability of the absorber. For undamped primary systems, closed-form solutions are available. Otherwise, tabulated values or fitting procedures can be applied.

In practical applications, the aforementioned theory is easily implementable. For the model presented in Section 3, there are a few limitations:

1. The compound vehicle/track/soil model is complex and intensive, requiring excessive computational time, especially in the case of a DVA optimization procedure.

2. A classical transfer function between the excitation and ground vibration is difficult to obtain since the excitation is moving; a traveling link between the vehicle and the track (not as an external force) must be defined and becomes nonlinear. Moreover, the ground vibration covers two contributions: a moving load effect (that can be considered as stationary) and the dynamic excitation at the wheel/defect interface (transient phenomenon).

To avoid using complex mathematical development in DVA tuning, this study does not consider the wheel/rail force as an internal excitation of the system but as an external force. The associated nonlinear Hertzian contact is not taken into account in the tuning procedure: a linearization is performed around the nominal wheel/rail force, providing a rapid way to fix the optimal values (a nonlinear behavior can be kept during the whole simulation). In addition, only the vehicle/track subsystem is used for the tuning procedure in the frequency domain. Once the values of φ_opt and ξ_opt are obtained for a fixed mass ratio μ, a full simulation can provide the ground vibration results in the time domain.

4.2 Numerical results

4.2.1 Frequency response function analysis

As previously mentioned, the tuning procedure is limited to the vehicle/track subsystem. As the vehicle/track interaction primarily affects the ground vibration, it is proposed to focus on the FRF of motorized wheels (in front of the leading car bogie and the central car bogie) with three different scenarios:

1. A DVA placed on the bogie (it is assumed that this location offers sufficient space for the device).

2. A DVA placed on the rail (close to the localized defect).

3. A DVA placed on the sleeper (underneath the localized defect).

Since both central and leading cars present different eigen-frequencies, it is recommended to study them separately. Practically, that means that two DVAs are necessary to suppress/attenuate the bogie bounce modes of the whole vehicle: one related to the leading car (at 19.6 Hz) and the other related to the central car (at 22.3 Hz). It is possible to observe their effect since vibrations induced by each car act separately (Fig. 4a).

Regarding the first scenario, various simulations confirmed that the best location of the DVA is on the bogie. Fig. 7 shows the calculated FRFs at the motorized wheel with and without the DVA. The mass value m_a is fixed to 200 kg, sufficiently realistic for

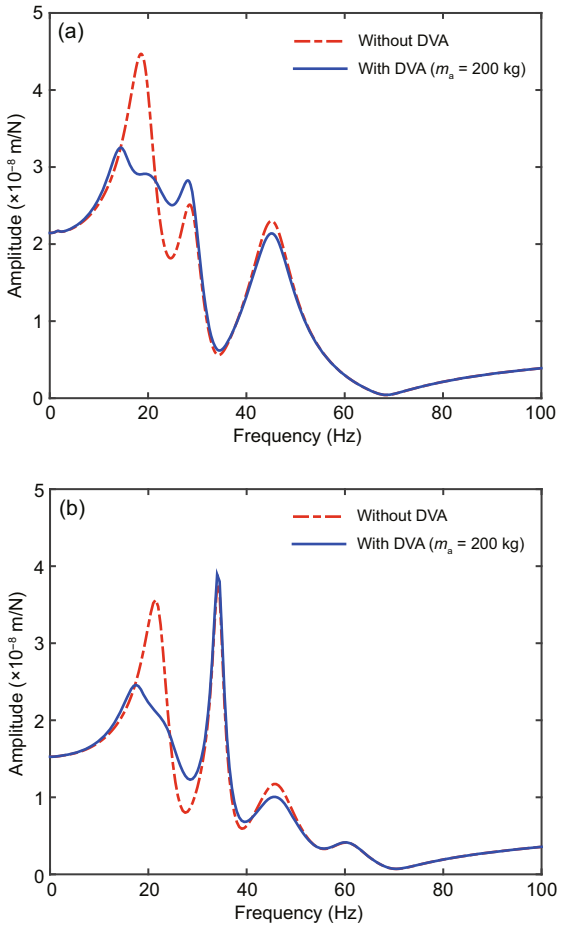

Fig. 7 Frequency response functions at the motorized wheel (driving point) with and without DVA of mass m_a = 200 kg at the vehicle bogie: excitation originated by the leading car (a) and the central car (b) configurations

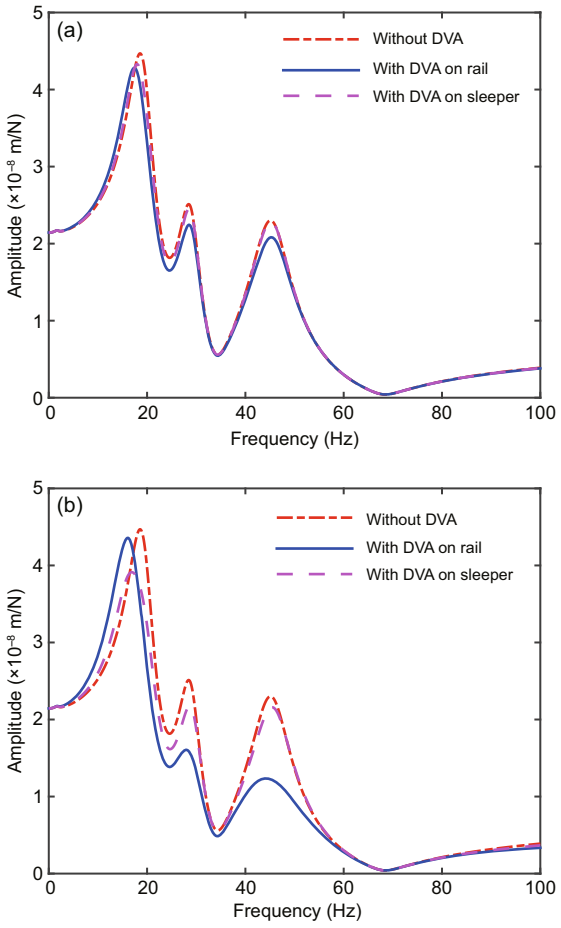

Fig. 8 Frequency response functions at the motorized wheel (driving point) with an excitation originated by the leading car for DVA placed on the track in the vicinity of the localized defect: (a) DVA mass of m_a = 200 kg; (b) DVA mass of m_a = 1000 kg

the present case. The last three vehicle modes, bogie bounce, bogie pitch, and axle hop modes, are visible (the first mode, car bounce mode, is not notably excited). In this particular study, the following DVA values were deduced: $k_a = 2.26$ MN/m and $c_a = 11.21$ kN·s/m (leading car with the tuned DVA frequency $f_a = 16.9$ Hz), and $k_a = 3.17$ MN/m and $c_a = 13.06$ kN·s/m (central car with $f_a = 20.0$ Hz). A clear amplitude reduction of around 2 dB is observed for these target bounce mode peaks without significantly modifying the other structure's modes (a minor amplitude reduction is observed for the axle hop mode, the fourth mode, around 45 Hz). For the leading bogie, the target mode is split into two modes at 14.87 Hz and 22.14 Hz, with increased levels of damping compared to the original mode (17.72 Hz and 25.08 Hz for the central car).

For the second configuration (scenarios 2 and 3), Fig. 8 presents the calculated FRFs considering the placement of the DVAs on the track for the leading car excitation. Two possible DVA masses were examined: $m_a = 200$ kg and $m_a = 1000$ kg. For the first results (Fig. 8a), it is observed that a minor variation is obtained for a DVA placed on the rail or on a sleeper. This is mainly due to the low DVA mass compared to the effective track mass: the effective mass provides a good picture of this property, since the mass ratio is relatively small ($\mu = 0.003$–0.006) compared to the aforementioned case ($\mu = 0.08$) with the same DVA mass. The second set of results (Fig. 8b) shows a greater attenuation for a DVA mass $m_a = 1000$ kg with notable differences between the rail and sleeper locations: for a DVA on the rail, the target resonance peak is less attenuated in favor of the other modes. With a DVA on the sleeper, it produces the opposite effect: the target resonance peak

is reduced considerably more.

Tables 3 and 4 provide additional results of the optimal values of the DVA parameters for different DVA masses for all studied scenarios. It is seen that the DVA damping and stiffness increase with the DVA mass and the natural frequency f_a of the DVA decreases with the mass. In a general way, the greater the DVA mass, the more the amplitude attenuation.

4.2.2 Ground vibration time history

Using the values in Tables 3 and 4, various simulations of the whole vehicle/track/soil model were performed in order to quantify the resulting ground vibration attenuation.

Fig. 9 presents the different results at free-field, for the observation point located at 2 m from the track, considering the case presented in Fig. 4b. Two DVA masses are analyzed: $m_a = 100$ kg and $m_a = 200$ kg. The impact of each bogie is separated in order to easily observe the effect of the DVA (front and rear leading cars induce the same ground vibration and thus only the front leading car is analyzed). From the time histories (Figs. 9a and 9b), it is shown that the DVA has a positive effect by modifying the ground vibration velocity shape and level. However, there is a small difference between the DVA mass cases, showing that increasing the DVA mass does not always result in greater amplitude reduction. Corresponding one-third octave band analysis confirms these observations by showing an effective reduction of the vibration magnitude around not only the target frequency, but also (to a lesser extent) at higher frequencies (as observed in the FRF results). Also, no notable difference between the two DVA masses is observed.

Fig. 10 (p.94) presents the root mean square (RMS) level calculated from the predicted time histories according to ISO 2631-2 (ISO, 2003) at various distances from the track. The different DVA configurations are retained: placed on the vehicle or on the track (sleeper). Although they are not presented, vibration levels in the case of a DVA placed on the rail provide very similar results to those for the DVA placed on a sleeper. Again, it is seen that the chosen DVA mass has an insignificant influence on the level, and is more pronounced for the DVA on the track. Compared to the solution of track location, a DVA placed on the vehicle remains a preferable solution in terms of vibration levels. Additional results for the central car confirm these observations.

5 Discussion and mitigation efficiency

From the analyzed results, several comments can be made regarding the implementation of a DVA in such applications. It is well established that a DVA placed on the vehicle is more efficient than that on the track. Economically speaking, since a particular vehicle such as the T2000 tram generates abnormal vibration on each singular geometry, it is advantageous to keep the DVA inside the vehicle rather than a DVA close to all rail defects. A design constraint could, however, limit the mass of the DVA when placed on the vehicle (mass and volume). There is less constraint for the track location (in

Table 3 Optimal values of DVA parameters for excitation generated by the leading car

Parameter	DVA on vehicle		DVA on rail			DVA on sleeper		
m_a(kg)	100	200	100	200	1000	100	200	1000
k_a(MN/m)	1.30	2.26	1.48	2.87	11.61	1.51	3.00	14.33
c_a(kN·s/m)	4.11	11.21	4.49	12.62	133.79	2.45	6.93	76.62
μ	0.080	0.160	0.014	0.029	0.144	0.003	0.006	0.030
f_a(Hz)	18.2	16.9	19.3	19.1	17.1	19.6	19.5	19.1

Table 4 Optimal values of DVA parameters for excitation generated by the central car

Parameter	DVA on vehicle		DVA on rail			DVA on sleeper		
m_a(kg)	100	200	100	200	1000	100	200	1000
k_a(MN/m)	1.77	3.17	1.95	3.80	15.98	1.99	3.97	19.56
c_a(kN·s/m)	4.75	13.06	4.63	13.01	139.27	2.16	6.11	68.08
μ	0.060	0.120	0.012	0.002	0.116	0.001	0.002	0.009
f_a(Hz)	21.2	20.0	22.2	21.9	20.1	22.4	22.4	22.3

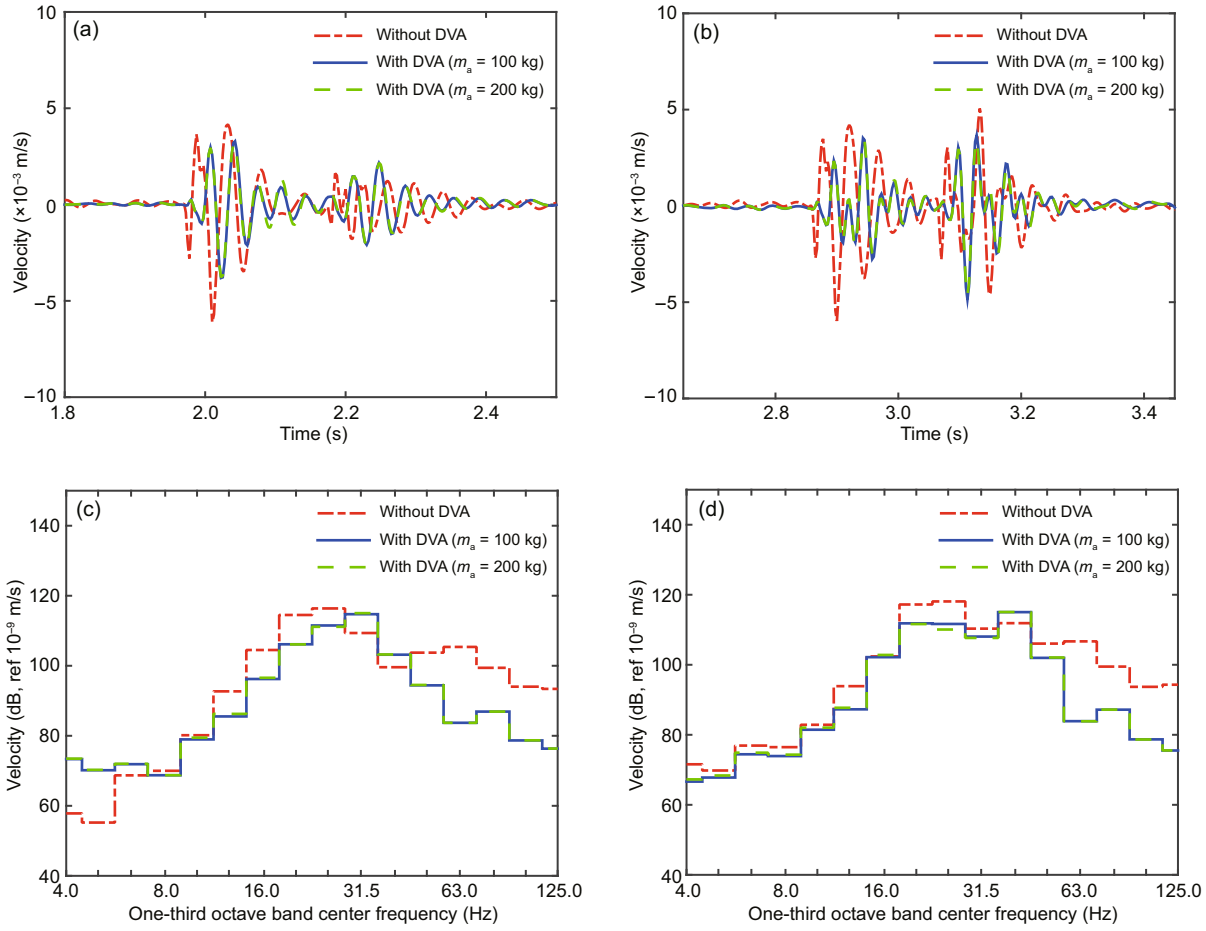

Fig. 9 Predicted vibration velocity at 2 m from the track due to the T2000 tram passing over a singular defect at a speed of 30 km/h: time history of the vibration induced by the leading car (a) and by the central car (b); corresponding frequency content of the vibration induced by the leading car (c) and by the central car (d)

terms of the mass). It was observed that an increase of DVA mass has no significant effect and a value of 100 kg provides satisfactory results.

Fig. 11 presents the relationship between the amplitude reduction ratio and the distance from the track, and includes an additional mitigation solution proposed by Kouroussis et al. (2012). This concerns the same vehicle but with a softer resilient material for the wheels (here the associated stiffness is divided by 8). By decreasing the resilient material stiffness, it is possible to obtain a significant amplitude reduction. This is explained by the beneficial effect of separating the unsprung mass (adding an additional connection layer results in a significant decoupling between the web and tread of the wheel) that enables the vibration transmission reduction from the wheel/track interaction to the vehicle. At first glance, compared to a softer resilient wheel, the DVA is less advantageous: the amplitude reduction across the studied distance 2–20 m is around 80% with a DVA, while a softer resilient wheel provides a reduction of approximately 50%.

It could be concluded that a DVA is less advantageous but, technically speaking, a softer resilient wheel has its own limitations, such as increased fragility and need for increased maintenance. In addition, if the wheels were to break, there are serious consequences that could be problematic for passengers, motorists, and people in the vicinity of the incident. Vehicle safety issues are less of a concern for a DVA placed on the bogie. Regarding the DVA, it is important to pay to the mechanical design of the DVA and particularly to its life span: a decrease of vibration amplitude of the primary system (vehicle) is often associated with vibration amplification in the auxiliary mass defining the DVA. It is

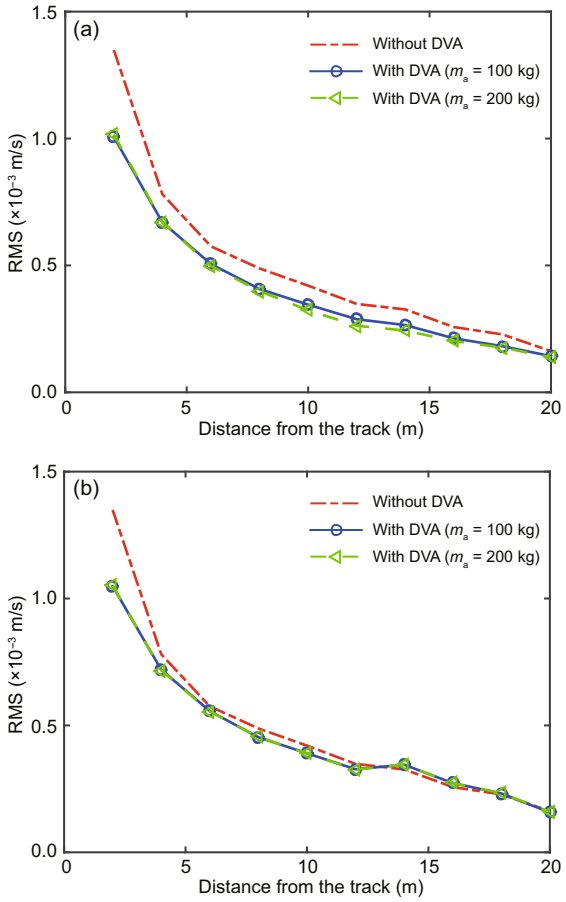

Fig. 10 RMS level as a function of the distance from the track related to the T2000 tram passing over a singular defect at a speed of 30 km/h due to: (a) the leading car; (b) the central car

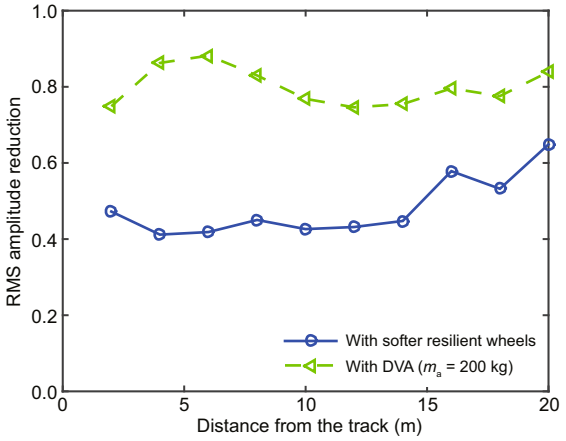

Fig. 11 Effect of mitigation measures on RMS amplitude reduction ratio (regarding amplitude reduction, 0.0 means 100% isolation, and 1.0 means 0% isolation)

important to consider that DVAs are subject to hard vibration and a dedicated and optimal design must take these factors into account.

This demonstrates the usefulness of a predictive model to aid the vehicle designer to determine suitable countermeasures to validate design methods. The parameters of a such system need to be determined in order to reliably predict the vibration transmission and to meet the expected vibration requirements, prior to any physical experiment.

6 Conclusions

The presence of low dampened vehicle modes strongly excited by localized defects induces severe vibration levels at the vicinity of tramway tracks. In order to alleviate such vibrations, it is proposed to design DVAs specifically tuned to a target frequency, namely the bogie bounce mode of the vehicle. A purely numerical approach is used to evaluate the potential of such mitigation measures in the case of urban conditions. The use of FRFs calculated from the vehicle/track was retained in order to calibrate the DVA parameters. The ground vibrations induced by a localized defect were afterwards calculated and compared to the frequency response analysis. The use of time-frequency analysis permitted the confirmation of a single main mode contributing to the ground vibrations. This was possible thanks to a direct correlation between the excitation forces and the ground vibration velocities on the time-frequency scale. The modal approach applied to the vehicle/track model offers a method to obtain the optimal DVA parameter values for any DVA location. Two locations were retained: the DVA placed on the vehicle (namely, on the bogie) and the DVA placed on the track (rail or sleeper close to the localized defect). It is found that a DVA placed on the vehicle, close to the excitation contributor and well tuned, provides an interesting solution to mitigate excessive levels of vibration in urban areas.

References

Ainalis D, Ducarne L, Kaufmann O, et al., 2018. Improved analysis of ground vibrations produced by man-made sources. *Science of the Total Environment*, 616-617:517-530. https://doi.org/10.1016/j.scitotenv.2017.10.291

Bruni S, Anastasopoulos I, Alfi S, et al., 2009. Train-induced vibrations on urban metro and tram turnouts. *Journal of Transportation Engineering*, 135(7):397-405. https://doi.org/10.1061/(asce)te.1943-5436.0000008

Cai CB, He QL, Zhu SY, et al., 2019. Dynamic interaction of suspension-type monorail vehicle and bridge: numerical

simulation and experiment. *Mechanical Systems and Signal Processing*, 118:388-407. https://doi.org/10.1016/j.ymssp.2018.08.062

Chen ZW, Fang H, Han ZL, et al., 2019. Influence of bridge-based designed TMD on running trains. *Journal of Vibration and Control*, 25(1):182-193. https://doi.org/10.1177/1077546318773022

Collette C, Horodinca M, Preumont A, 2009. Rotational vibration absorber for the mitigation of rail rutting corrugation. *Vehicle System Dynamics*, 47(6):641-659. https://doi.org/10.1080/00423110802339792

Connolly D, Giannopoulos A, Fan W, et al., 2013. Optimising low acoustic impedance back-fill material wave barrier dimensions to shield structures from ground borne high speed rail vibrations. *Construction and Building Materials*, 44:557-564. https://doi.org/10.1016/j.conbuildmat.2013.03.034

Connolly DP, Marecki GP, Kouroussis G, et al., 2016. The growth of railway ground vibration problems–a review. *Science of the Total Environment*, 568:1276-1282. https://doi.org/10.1016/j.scitotenv.2015.09.101

Coulier P, François S, Degrande G, et al., 2013. Subgrade stiffening next to the track as a wave impeding barrier for railway induced vibrations. *Soil Dynamics and Earthquake Engineering*, 48:119-131. https://doi.org/10.1016/j.soildyn.2012.12.009

de Roeck G, Degrande G, Dewulf W, et al., 1996. Design of a vibration isolating screen. *In*: Topping BHV (Ed.), Advances in Finite Element Technology. Civil-Comp Press, Edinburgh, UK, p.379-385. https://doi.org/10.4203/ccp.39.9.5

Den Hartog JP, 1985. Mechanical Vibrations (4th Edition). Courier Corporation, McGraw-Hill, New York, USA.

Germonpré M, Degrande G, Lombaert G, 2018. Periodic track model for the prediction of railway induced vibration due to parametric excitation. *Transportation Geotechnics*, 17:98-108. https://doi.org/10.1016/j.trgeo.2018.09.015

Gong D, Zhou JS, Sun WJ, 2013. On the resonant vibration of a flexible railway car body and its suppression with a dynamic vibration absorber. *Journal of Vibration and Control*, 19(5):649-657. https://doi.org/10.1177/1077546312437435

Grassie SL, Elkins JA, 1997. Rail corrugation on North American transit systems. *Vehicle System Dynamics*, 29(S1):5-17. https://doi.org/10.1080/00423119708969548

Grossoni I, Iwnicki S, Bezin Y, et al., 2015. Dynamics of a vehicle–track coupling system at a rail joint. *Proceedings of the Institution of Mechanical Engineers, Part F: Journal of Rail and Rapid Transit*, 229(4):364-374. https://doi.org/10.1177/0954409714552698

ISO (International Organization for Standardization), 2003. Mechanical Vibration and Shock—Evaluation of Human Exposure to Whole-body Vibration—Part 2: Vibration in Buildings (1 Hz to 80 Hz), ISO 2631-2:2003. ISO, Geneva, Switzerland.

Kaewunruen S, Martin V, 2018. Life cycle assessment of railway ground-borne noise and vibration mitigation methods using geosynthetics, metamaterials and ground improvement. *Sustainability*, 10(10):3753. https://doi.org/10.3390/su10103753

Kouroussis G, Verlinden O, 2013. Prediction of railway induced ground vibration through multibody and finite element modelling. *Mechanical Sciences*, 4(1):167-183. https://doi.org/10.5194/ms-4-167-2013

Kouroussis G, Verlinden O, 2015. Prediction of railway ground vibrations: accuracy of a coupled lumped mass model for representing the track/soil interaction. *Soil Dynamics and Earthquake Engineering*, 69:220-226. https://doi.org/10.1016/j.soildyn.2014.11.007

Kouroussis G, Verlinden O, Conti C, 2010. On the interest of integrating vehicle dynamics for the ground propagation of vibrations: the case of urban railway traffic. *Vehicle System Dynamics*, 48(12):1553-1571. https://doi.org/10.1080/00423111003602392

Kouroussis G, Gazetas G, Anastasopoulos I, et al., 2011. Discrete modelling of vertical track–soil coupling for vehicle–track dynamics. *Soil Dynamics and Earthquake Engineering*, 31(12):1711-1723. https://doi.org/10.1016/j.soildyn.2011.07.007

Kouroussis G, Verlinden O, Conti C, 2012. Efficiency of resilient wheels on the alleviation of railway ground vibrations. *Proceedings of the Institution of Mechanical Engineers, Part F: Journal of Rail and Rapid Transit*, 226(4):381-396. https://doi.org/10.1177/0954409711429210

Kouroussis G, van Parys L, Conti C, et al., 2013. Prediction of ground vibrations induced by urban railway traffic: an analysis of the coupling assumptions between vehicle, track, soil, and buildings. *International Journal of Acoustics and Vibration*, 18(4):163-172. https://doi.org/10.20855/ijav.2013.18.4330

Kouroussis G, Connolly DP, Verlinden O, 2014. Railway-induced ground vibrations–a review of vehicle effects. *International Journal of Rail Transportation*, 2(2):69-110. https://doi.org/10.1080/23248378.2014.897791

Kouroussis G, Connolly DP, Alexandrou G, et al., 2015. Railway ground vibrations induced by wheel and rail singular defects. *Vehicle System Dynamics*, 53(10):1500-1519. https://doi.org/10.1080/00423114.2015.1062116

Kouroussis G, Vogiatzis KE, Connolly DP, 2018. Assessment of railway ground vibration in urban area using in-situ transfer mobilities and simulated vehicle-track interaction. *International Journal of Rail Transportation*, 6(2):113-130. https://doi.org/10.1080/23248378.2017.1399093

Licitra G, Fredianelli L, Petri D, et al., 2016. Annoyance evaluation due to overall railway noise and vibration in Pisa urban areas. *Science of the Total Environment*,

568:1315-1325.
https://doi.org/10.1016/j.scitotenv.2015.11.071

Mandal NK, Dhanasekar M, Sun YQ, 2016. Impact forces at dipped rail joints. *Proceedings of the Institution of Mechanical Engineers, Part F: Journal of Rail and Rapid Transit*, 230(1):271-282.
https://doi.org/10.1177/0954409714537816

Morys B, Kuntze HB, 1997. Simulation analysis and active compensation of the out-of-round phenomena at wheels of high speed trains. Proceedings of World Congress on Railway Research, p.16-19.

Nielsen JCO, Mirza A, Cervello S, et al., 2015. Reducing train-induced ground-borne vibration by vehicle design and maintenance. *International Journal of Rail Transportation*, 3(1):17-39.
https://doi.org/10.1080/23248378.2014.994260

Paixão A, Fortunato E, Calçada R, 2015. Design and construction of backfills for railway track transition zones. *Proceedings of the Institution of Mechanical Engineers, Part F: Journal of Rail and Rapid Transit*, 229(1):58-70.
https://doi.org/10.1177/0954409713499016

Steffen Jr V, Rade D, 2001. Vibration absorbers. *In*: Braun S (Ed.), Encyclopedia of Vibration. Elsevier, Oxford, UK, p.9-26.

Talbot JP, 2014. Lift-over crossings as a solution to tram-generated ground-borne vibration and re-radiated noise. *Proceedings of the Institution of Mechanical Engineers, Part F: Journal of Rail and Rapid Transit*, 228(8):878-886.
https://doi.org/10.1177/0954409713499015

Thompson DJ, Jones CJC, Waters TP, et al., 2007. A tuned damping device for reducing noise from railway track. *Applied Acoustics*, 68(1):43-57.
https://doi.org/10.1016/j.apacoust.2006.05.001

Uzzal RUA, Ahmed W, Bhat RB, 2016. Impact analysis due to multiple wheel flats in three-dimensional railway vehicle-track system model and development of a smart wheelset. *Proceedings of the Institution of Mechanical Engineers, Part F: Journal of Rail and Rapid Transit*, 230(2):450-471.
https://doi.org/10.1177/0954409714545558

Vincent N, Bouvet P, Thompson DJ, et al., 1996. Theoretical optimization of track components to reduce rolling noise. *Journal of Sound and Vibration*, 193(1):161-171.
https://doi.org/10.1006/jsvi.1996.0255

Vogiatzis K, 2012. Protection of the cultural heritage from underground metro vibration and ground-borne noise in Athens centre: the case of Kerameikos Archaeological Museum and Gazi Cultural Centre. *International Journal of Acoustics and Vibration*, 17(2):59-72.
https://doi.org/10.20855/ijav.2012.17.2301

Vogiatzis K, Mouzakis H, 2018. Ground-borne noise and vibration transmitted from subway networks to multi-storey reinforced concrete buildings. *Transport*, 33(2):446-453.
https://doi.org/10.3846/16484142.2017.1347895

Vogiatzis K, Zafiropoulou V, Mouzakis H, 2018. Monitoring and assessing the effects from metro networks construction on the urban acoustic environment: the Athens metro line 3 extension. *Science of the Total Environment*, 639:1360-1380.
https://doi.org/10.1016/j.scitotenv.2018.05.143

Zhai WM, Wang KY, Cai CB, 2009. Fundamentals of vehicle–track coupled dynamics. *Vehicle System Dynamics*, 47(11):1349-1376.
https://doi.org/10.1080/00423110802621561

Zhu SY, Yang JZ, Cai CB, et al., 2017a. Application of dynamic vibration absorbers in designing a vibration isolation track at low-frequency domain. *Proceedings of the Institution of Mechanical Engineers, Part F: Journal of Rail and Rapid Transit*, 231(5):546-557.
https://doi.org/10.1177/0954409716671549

Zhu SY, Wang JW, Cai CB, et al., 2017b. Development of a vibration attenuation track at low frequencies for urban rail transit. *Computer-Aided Civil and Infrastructure Engineering*, 32(9):713-726.
https://doi.org/10.1111/mice.12285

Appendix A: Details of the measured and calculated parameters: vehicle, track, and soil

The T2000 tram has the following dynamic properties:

1. Front or rear leading car body mass $m_c = 7580\,\mathrm{kg}$.

2. Central car body mass $m_c = 2600\,\mathrm{kg}$.

3. Bogie mass (leading or central car) $m_b = 1800\,\mathrm{kg}$ and pitch inertia $I_b = 300\,\mathrm{kg{\cdot}m^2}$.

4. Independent motor wheel mass $m_m = 945\,\mathrm{kg}$ with a tread of $m_t = 80\,\mathrm{kg}$ and a resilient material of stiffness $k_t = 145\,\mathrm{MN/m}$ and damping $c_t = 3\,\mathrm{kN{\cdot}s/m}$.

5. Trailer wheel mass $m_d = 160\,\mathrm{kg}$.

6. Primary suspension (trailer wheels) of stiffness $k_d = 5.88\,\mathrm{MN/m}$ and damping $c_d = 6\,\mathrm{kN{\cdot}s/m}$.

7. Primary suspension (motor wheels) of stiffness $k_m = 44\,\mathrm{MN/m}$ and damping $c_m = 18\,\mathrm{kN{\cdot}s/m}$.

8. Secondary suspension of stiffness $k_2 = 960\,\mathrm{kN/m}$ and damping $c_2 = 56.25\,\mathrm{kN{\cdot}s/m}$.

Table A1 presents track and foundation parameters. More information about the CLM model (and the associated parameters) can be obtained from Kouroussis et al. (2011). The soil is represented by visco-elastic behavior according to a six-horizontal layer configuration. Table A2 presents the values.

Table A2 Soil characteristics and layering

Position	Young's modulus (MPa)	Density (kg/m^3)	Poisson's ratio	Viscous damping (ms)	Depth (m)
Layer 1	61	1876	0.13	0.4	1.2
Layer 2	84	1876	0.13	0.4	1.8
Layer 3	287	1876	0.13	0.4	1.0
Layer 4	373	1876	0.27	0.4	1.0
Layer 5	450	1876	0.33	0.4	1.0
Halfspace	465	1992	0.48	0.4	–

Table A1 Track properties

Parameter	Value
Rail flexural stiffness, $E_\mathrm{r}I_\mathrm{r}$ (MN·m^2)	4.17
Rail mass per length, $\rho_\mathrm{r}A_\mathrm{r}$ (kg/m)	54
Sleeper spacing, L (m)	0.72
Railpad stiffness, k_p (MN/m)	90
Railpad damping, c_p (kN·s/m)	30
Ballast stiffness, k_b (MN/m)	32
Ballast damping, c_b (kN·s/m)	52
Foundation mass, m_f (kg)	2502
Direct foundation stiffness, k_f (MN/m)	30
Coupling foundation stiffness, k_c (MN/m)	41
Direct foundation damping, c_f (kN/m)	150
Coupling foundation damping, c_c (kN/m)	−23

Introducing Editorial Board Member:

Dr. Georges KOUROUSSIS has been the Editorial Board Member of *Journal of Zhejiang University-SCIENCE A (Applied Physics & Engineering)* since 2016.

Dr. Georges KOUROUSSIS obtained his master degree in mechanical engineering from the Faculty of Engineering of Mons, Belgium, in June 2002. He earned a PhD in applied sciences on railway-induced ground vibrations in May 2009. In 2010, he was an invited postdoctoral researcher at the National Technical University of Athens (NTUA–Greece).

He currently works as a senior lecturer/associate professor in the Department of Theoretical Mechanics, Dynamics, and Vibrations at the University of Mons, Belgium. He takes part in the theoretical mechanics and dynamics labs, exercises, and courses. His experience covers experimental work, theoretical and numerical analysis and design, from across a wide range of expertise in industry. He is a member of the American Society of Mechanical Engineers (ASME), the International Institute of Acoustics and Vibrations (IIAV), the European Association for Structural Dynamics (EASD), the Association Française de Mécanique (AFM), and the European Mechanics Society (EUROMECH).

Dr. KOUROUSSIS' current research activities include railway-induced ground vibrations, blast-induced ground vibrations, geotechnical testing and engineering, dynamic analysis of complex structures, and vibration signal processing. He has been recently elected director of the IIAV for the period 2016–2020.

中文概要

题　目：轨道局部缺陷引起的城市轨道交通地面振动——应用动力吸振器作为减振措施

目　的：基于动力吸振器理论提出一种控制城市轨道交通地面振动的有效措施。

创新点：1. 确定动力吸振器安装在车辆或轨道上的最优位置和动力学参数；2. 采用提出的两步分析法真实模拟布鲁塞尔有轨电车在通过轨道局部缺陷时引起的地面振动；3. 探明动力吸振器安装在车辆或轨道上对控制地面振动的有效性。

方　法：1. 通过对列车–轨道耦合动力学系统进行模态分解，得出在不同位置安装动力吸振器的最优动力学参数；2. 采用所提出的两步法预测不同工况下城市轨道交通的地面振动：首先建立多体车辆与轨道耦合动力学模型，计算作用在土体上的动力作用，然后建立三维土体有限元模型，模拟动力作用引起的地面波传播及周边的地面振动。

结　论：将动力吸振器安装在车辆上是降低城市轨道交通地面振动的有效措施。

关键词：动力吸振器；道岔；钢轨接头；地面振动；布鲁塞尔有轨电车